Surface-enhanced Raman spectroscopy substrate fabricated via nanomasking technique for biological sensor applications

Stephen J. Bauman[a], Ahmad A. Darweesh[a], Joseph B. Herzog[*,a,b]

[a]Microelectronics-Photonics Program, University of Arkansas, Fayetteville, AR, 72701, USA;
[b]Department of Physics, University of Arkansas, Fayetteville, AR, 72701, USA;

ABSTRACT

The nanomasking fabrication technique has been shown to be capable of producing many sub-10 nm gaps between metallic structures over a wafer-scale area. This provides the opportunity to utilize the technique in spectroscopy signal enhancement applications. Here we describe a device designed via nanomasking that holds potential as a surface enhanced Raman spectroscopy (SERS) substrate for biosensing or other applications. The high density of plasmonic hotspot nanogaps improves the feasibility of these types of patterns for signal enhancement, as it provides ease of use and increased speed of sample deposition for taking spectrum. The ability to fabricate these patterns with high repeatability at mass production scale is another benefit of nanomasking-fabricated spectroscopy substrates. This work demonstrates tests of fabricated devices for use in a custom Raman spectroscopy system as a potential source of signal enhancement. Also, theoretical enhancement results are calculated for comparison via computational electromagnetic studies.

Keywords: Plasmon, nanogap, sub-10nm, nanofabrication, scalable nano, Raman, plasmonic enhancement, SERS

1. INTRODUCTION

Nanoscale optical phenomena have been studied for decades, and they are currently an attractive topic of research and technological development. This field refers to the study of material geometries smaller than the wavelength of light incident upon them, specifically with dimensions between 1 and 100 nm. Electronic oscillations known as plasmons on the surface of conducting materials are caused by the incident light's electric field, and, at this scale, are able to resonate along the length of the nanostructures without significant decay. The resulting electric fields from the regions of high and low charge concentration near the material surface are capable of producing a net increase in the electric field versus that of the incident light. This is known as plasmonic enhancement, and many studies have shown the benefit of various metallic geometries on a substrate for the purpose of creating near-field optical enhancement, or local electric field divided by incident field strength all squared, $(E/E_0)^2$.[1–3]

Existing and potential applications of plasmonic enhancement include improved photovoltaics,[4–11] enhanced biomedical agent detection and diagnostics,[12–18] and precision chemical detection to the point of single molecule detection.[19–22] The latter two often make use of enhance spectroscopy techniques using plasmonic particles or structures to improve the signal emitted from a sample during a test. Surface-enhanced Raman spectroscopy (SERS) is one example of using substrates altered with plasmonically active structures to obtain a stronger signal from what may otherwise be an undetectable source.[23–29] Increased sensitivity of detecting different chemical agents in a sample is crucial to improving field tests for various diseases and medical conditions. The stronger and more reliable the signal enhancement, the simpler it becomes to provide cost effective devices to users across the globe where medical diagnoses can be truly life-saving.

In addition to nanostructures producing electric field enhancement, gaps between structures, specifically those approaching 10 nm and smaller,[30] have been shown to produce an even stronger field multiplication.[31–35] These nanogaps are able to contain "hotspots" of much higher field strength due to coupling of the plasmons from the adjacent structures. Studies of these hotspots as the key component in SERS substrates have shown promising results.[36–38] One limitation of using sub-10 nm gaps for plasmonic enhancement in various applications is the difficulty of reliably fabricating them.

Prior work demonstrating the success of nanogap structures for SERS and other plasmonic applications have, in many cases, been limited to testing the effects of single, isolated gaps. Many techniques for fabricating gaps can only create

* Email: jbherzog@uark.edu

Advanced Fabrication Technologies for Micro/Nano Optics and Photonics IX, edited by Georg von Freymann, Winston V. Schoenfeld, Raymond C. Rumpf, Proc. of SPIE Vol. 9759, 97591I
 · doi: 10.1117/12.2213086

them in series, making it an arduous process to pattern many gaps across a substrate surface. The nanomasking technique, as outlined by Bauman et al.,[39] overcomes this limitation via a unique multistep lithography process in order to simultaneously produce many sub-10 nm gaps across a surface. Nanomasking provides the experimenter with wide geometrical fabrication freedom,[40,41] and thus presents itself as an ideal candidate for patterning SERS substrates for something such as a biosensing application.

2. NANOMASKING GRID STRUCTURES

The nanomasking process was chosen to pattern structures to be tested for efficacy as SERS substrates. The ability to create multiple nanogaps simultaneously was desirable, as an increase in the number of plasmonic hotspots was hypothesized to improve the chances of obtaining a detectable signal.

2.1 Fabrication Process

As described by Bauman et al.[39], the nanomasking process is a two-step lithography process. The first step, using electron beam lithography (EBL) or photolithography, patterns the desired primary geometry. In this work, EBL was used, and electron beam evaporation was used to deposit the materials (1.4 nm Ti, 14 nm Au, 1.4 nm SiO_2, and 14 nm Cr), though other deposition methods may also function. The Cr was allowed to oxidize, resulting in a parallel nanowire pattern as shown in Fig. 1(a) (only Au and Cr_xO_y are shown). The second lithography pattern consisted of more parallel rectangles, only these were perpendicular to the primary nanowires. The secondary evaporation of Ti and Au resulted in a sample with overlapping nanowires as seen in Fig. 1(b) (only Au is shown). Upon etching away the Cr_xO_y and the Au on top, the resulting structure was a grid of nanowires with sub-10 nm gaps separating the Au structures at each intersection (Fig. 1(c)).[41]

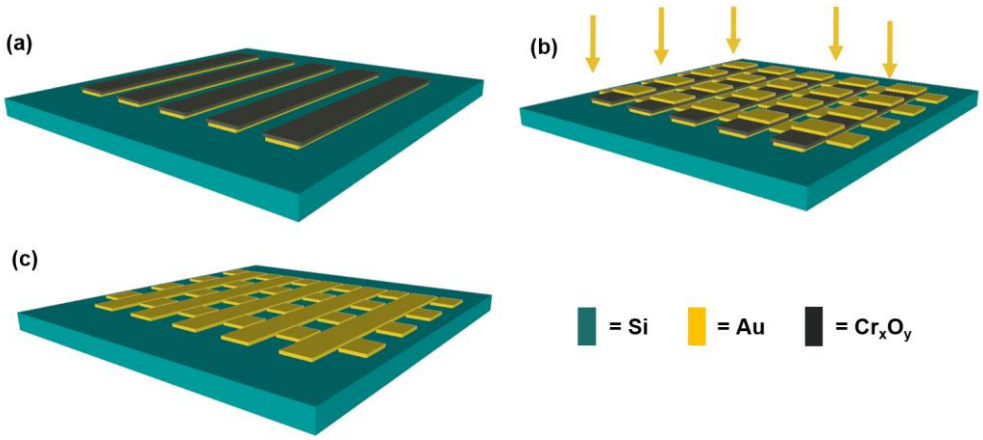

Figure 1. 3D sketch of the nanomasking fabrication process for creating a grid pattern with multiple nanogap hotspots over a substrate area. (a) Result of the first lithography step and deposition showing wires of Au topped with Cr_xO_y. (b) Result of the second lithography step and deposition showing overlapping wires of Au masked by Cr_xO_y. (c) Result of etching Cr_xO_y showing Au wire grid with nanogaps between adjacent wires. Adapted from Bauman.[41]

This design was chosen for the high density of resulting nanogaps and for the ability to control the resulting widths of both orientations of nanowires individually. None of these preliminary design widths were based on electromagnetic simulation results, and so were not necessarily optimized for plasmonic enhancement.

2.2 Fabrication Results

Nanomasking was successful in fabricating the grid structures as designed and as outlined in Fig. 1. Scanning electron microscopy (SEM) images were taken of the resulting structures and are shown in Fig. 2. Different design widths and spacings of the primary nanowires were found to produce different widths of the adjacent secondary Au structures. With the designs producing a resulting primary width of 165 nm, secondary structures were measured to be 65 nm as shown in Fig. 2(a) and (b). A slightly larger primary width of 180 nm resulted in a secondary structure width of 55 nm (Fig. 2(c)). Further increasing to a primary of 200 nm gave a 40 nm secondary (Fig. 2(d)). From previous measurements on nanomasking results using the same fabrication parameters as in this work, the median gap width was approximately 8.21 nm with a standard deviation of 3.03 nm.[39]

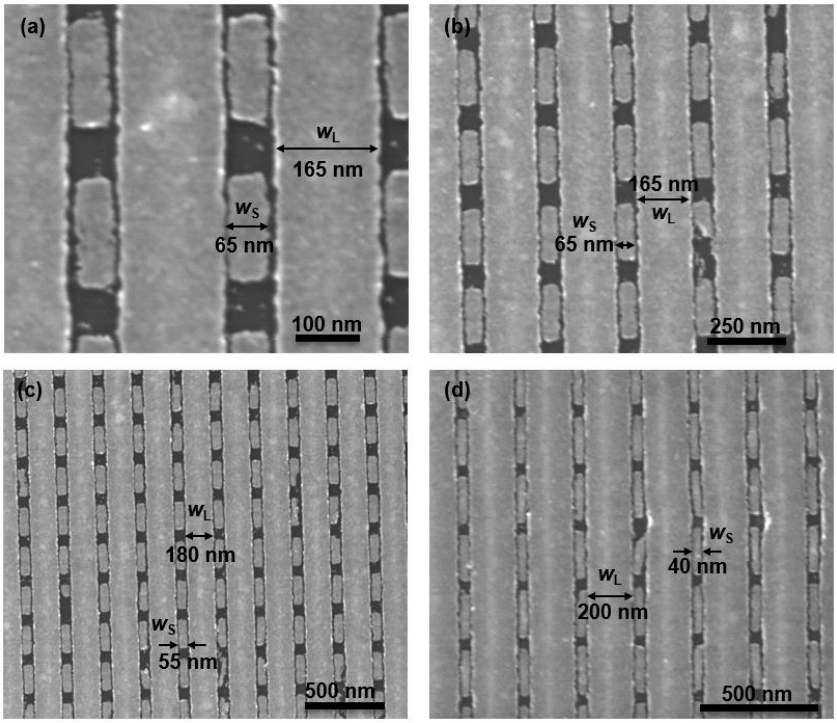

Figure 2. SEM images of dual-width grid structures fabricated using nanomasking with different designed wire widths. The width and spacing of the large wires, w_L, controls the width of the adjacent wires, w_S. (a) and (b) w_S = 65 and w_L = 165. (c) w_S = 55 and w_L = 180. (d) w_S = 40 and w_L = 200. All measurements are assumed to have a standard deviation of 3.03 nm.[39]

The fact that adjusting the primary Au structure width demonstrates the tunability of the resulting grids via the nanomasking technique. This will prove useful in future experiments by allowing designers to strategically pattern geometries that show optimal enhancement in simulations. This will accelerate the learning process in determining the efficiency of the grid structures as SERS substrates.

3. RAMAN SPECTROSCOPY

3.1 Experimental Setup

Raman spectroscopy works by shining an incident laser beam onto a sample and collecting the scattered light, due to inelastic scattering. The spectrometer collects light scattered back through the system, and inelastically scattered light acts as a fingerprint of the specific chemicals present in a sample due to their unique vibrational modes. The experimental Raman spectroscopy setup is shown in Fig. 3. The incident light source is a 100 mW, 785 nm (near-infrared), continuous-wave, unpolarized laser. The beam may pass through a 3.0 optical density filter or attenuator on a flip mount in order to sufficiently attenuate the beam for imaging. A linear polarizer and rotating half wave plate allow for tests of polarization dependence. The then polarized laser beam is reflected by a dichroic beam splitter and passes through a 50× objective, where it scatters off the sample. The sample is mounted on an x-y-z stage to aid in alignment and focusing. The scattered beam passes through the sharp-edge long-pass dichroic beam splitter. The remaining beam is then sharply attenuated for the 785 nm wavelength and below. Another flip-mounted long-pass filter further attenuates the laser wavelength, allowing longer wavelength Stokes peaks to pass through. The beam either reflects off a mirror and into a CMOS camera for imaging or passes straight through a focusing lens and into the Princeton Instruments Acton SP2500 spectrometer to produce experimental data.

For bright-field imaging of the sample and aligning the beam, the optical density filter is flipped into the beam path and the long pass filter is flipped out of the way in order to optimally image the beam. A white LED light source is incident on the sample using a Köhler illumination system. The 50/50 beam splitter passes the beam and reflected white light to the mirror where it is reflected into the CMOS camera. During spectroscopy, the 50/50 beam splitter is removed, the attenuator and mirror to the CMOS are flipped out of the way of the beam, and the long pass filter is flipped into the beam

path. Spectrometer settings such as slit width and exposure time were varied slightly, but typically, the slit was opened by 200 µm for 0.5 s with the 300 gr/mm diffraction grating selected.

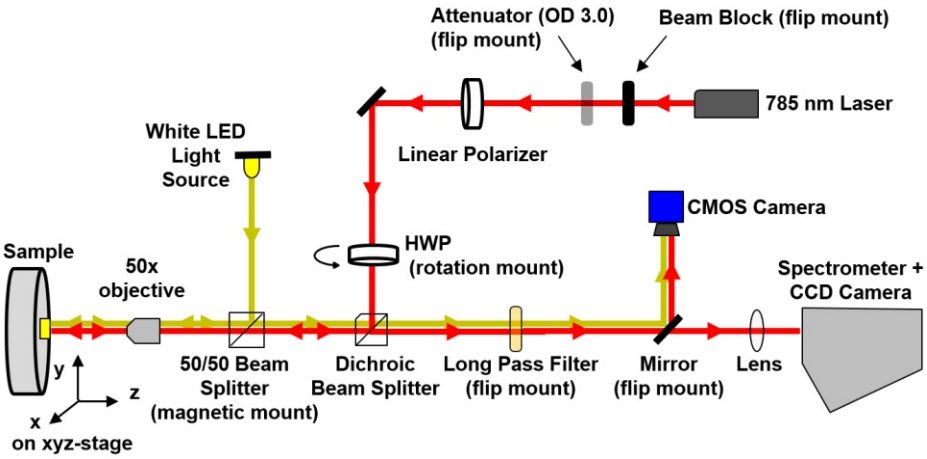

Figure 3. Depiction of the custom Raman spectroscopy setup to be used in SERS experiments with samples created via nanomasking. A 100 mW 785 nm near-infrared continuous-wave unpolarized laser is used for spectroscopy, with a white LED Köhler illumination setup and CMOS camera used for imaging and aligning the sample.

The data from the spectrometer can be shifted to remove the remnants of the filtered laser peak so that the scattered peaks become more visible. This shows the Stokes Raman peaks of materials present in the sample with signals strong enough to be observed at the corresponding relative wavenumbers.

3.2 Preliminary Results

Preliminary results were obtained using this custom Raman setup by testing a bare Si wafer. The Stokes Raman peak for Si was found at approximately 528 cm^{-1}, corresponding to the expected value. A plot of the spectrum obtained via the custom experimental setup is shown in Fig. 4.

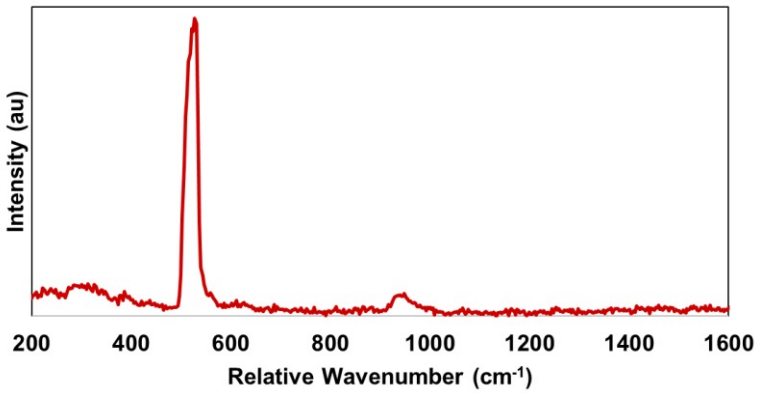

Figure 4. Preliminary data obtained from a Si sample on the custom Raman spectroscopy setup showing the Stokes Raman peak for Si at a relative wavenumber of 528 cm^{-1}.

The success of conducting Raman spectroscopy experiments with the setup described in this work was demonstrated by this initial test, and these results have been highly repeatable. Preliminary tests will use polymer 1,2-Di(4-pyridyl)ethylene, 97% (BPE) drop-casted onto samples containing the grid structures as shown in Fig. 2.

4. PLASMONIC ENHANCEMENT

4.1 Multiple Hotspots

One key benefit of the nanowire grid or other designs made possible to fabricate by the nanomasking technique is that a high density of many nanogaps can be created over a large area. Unlike some methods such as electromigration[36,42] and mechanical break junctions,[37,43] nanomasking creates many plasmonic hotspots that can increase a SERS signal. This is highly beneficial in SERS for biomedical applications, as speed and repeatability are crucial. The importance of multiple hotspots comes from the likelihood of the molecule to be detected making its way to the vicinity of a nanogap. If there is a low density of gaps and molecules, there is a lower chance of any molecules being present near a hotspot. With a substrate containing a high density of nanogaps, lower densities of the desired molecule can be detected.

Another benefit of a sample containing many nanogaps is that a diffraction-limited Gaussian laser beam need not be aligned so precisely in order to be sure of its illumination of a gap. As illustrated in Fig. 5, a beam focused to a diffraction-limited spot may be capable of illuminating multiple nanogaps, creating multiple plasmonic hotspots. These active hotspots may then all contribute to a SERS signal, versus having a single gap perform the action.

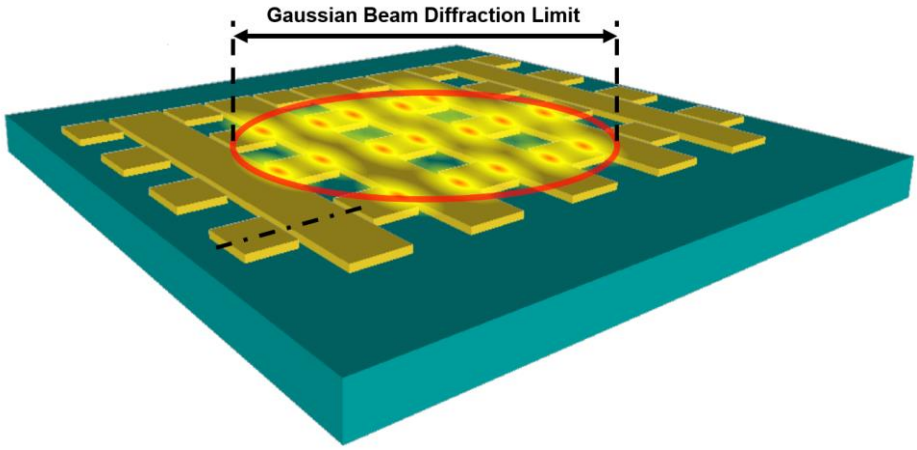

Figure 5. 3D sketch of a grid structure showing illumination over the area of a diffraction-limited Gaussian beam spot causing multiple hotspots due to the presence of nanogaps.

4.2 Electromagnetic Simulations

In order to optimize the strength of the hotspots in the gaps between structures capable of being fabricated via nanomasking, computational electromagnetic simulations were conducted. The geometry was chosen as a cross section of the Fig. 5 sketch as shown by the dashed cut line in the figure. The nanowire widths were set to match those of structures fabricated as shown in the SEM images in Fig. 2(a) and (b). A charge distribution plot and an electric field distribution plot are shown in Fig 6(a) and (b), respectively, where w_L = 165 nm and w_S = 65 nm. The nanowires were set to have the material parameters of Au, and the surrounding medium was an effective medium designed to simulate the Si substrate and the air above the surface. The effective refractive index, n_{eff}, was set at 1.25. Electromagnetic radiation with a wavelength of 785 nm was simulated to irradiate the surface from above, matching how the Raman laser strikes the sample.

The resulting charge distribution and electric field distribution plots show the presence of increased electric field within the gap, as was expected. The peak optical enhancement, or the local electric field divided by the incident field strength all squared $(E/E_0)^2$, was 221 in the gap. The presence of gaps alone, however, does not mean that the geometry will produce the optimal electric field increase. There may be a better combination of nanowire widths to simulate as well as to fabricate in the hopes of measuring a strong SERS signal from this grid structure. Additional simulations will be used to optimize the grid structure design in order to obtain the strongest enhancement. This will be crucial to the development of a functional SERS substrate and future developments.[44]

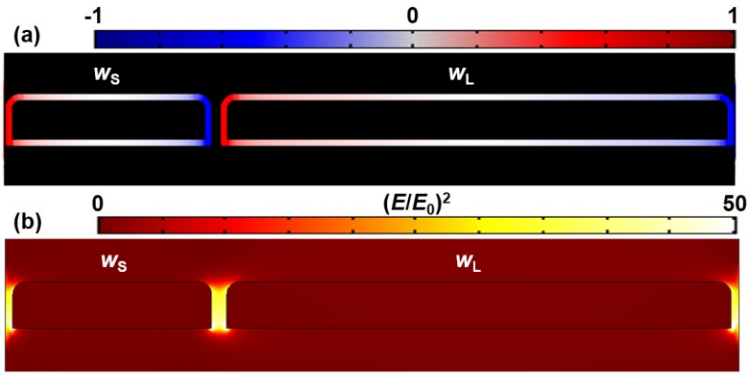

Figure 6. Simulation results of a cross section taken as shown by the cut in Fig. 5 with w_L = 165 nm and w_S = 65 nm as shown in SEM images in Fig. 2. (a) Charge distribution and (b) electric field distribution at 785 nm incident wavelength. Color bars indicate the normalized linear charge distribution and electric field enhancement $(E/E_0)^2$. The Si substrate is simulated by using an effective medium, n_{eff} = 1.25, surrounding the Au, and so is not shown.

5. CONCLUSIONS

This work demonstrates the successful fabrication of SERS substrates via the nanomasking technique, preliminary Raman spectroscopy experiments, and simulation results for the geometries fabricated. The nanomasking technique continues to exhibit repeatability in producing metallic nanogap structures of various geometries. Nanowire grids with sub-10 nm gaps at every intersection hold the potential to provide many plasmonic hotspots for use in a spectroscopy enhancing application, as confirmed by electromagnetic simulation of the structures. Fabrication results demonstrated hotspot density of 5×10^8 /cm^2. A custom Raman spectroscopy setup was built and tested successfully using a bare Si wafer, the result being a highly visible Si Stokes Raman peak. Initial SERS tests have been performed using the fabricated grid structures, but it appears that more optimization of the geometries will help produce a stronger plasmonic enhancement to aid in detecting chemical signatures. Further simulations of dual-width nanowire geometries will be crucial to this optimization process.

ACKNOWLEDGEMENTS

We would like to acknowledge the following colleagues at the University of Arkansas for all of their help and support: Plasmonic Nano-Optics group members David French, Gabi Abraham, Mirsaeid Sarollahi, Desalegn Debu, Pijush Ghosh, and Avery Hill as well as other colleagues Ahmad Nusir, Richard Penhallegon, and Brandon Rogers. We would also like to thank Joe Nabity for his technical support with the NPGS software. This work has been supported by funding from the Arkansas Biosciences Institute. Stephen J. Bauman has been supported by the Doctoral Academy Fellowship through the University of Arkansas Graduate School and the SPIE Optics + Photonics Education Scholarship, and travel funding for this presentation has been provided by the University of Arkansas Graduate School travel grant.

REFERENCES

[1] Barnes, W. L., Dereux, A.., Ebbesen, T. W., "Surface plasmon subwavelength optics," Nature **424**(6950), 824–830 (2003).
[2] Zayats, A. V., Smolyaninov, I. I.., Maradudin, A. A., "Nano-optics of surface plasmon polaritons," Phys. Rep. **408**(3–4), 131–314 (2005).
[3] Halas, N. J., "Plasmonics: An Emerging Field Fostered by Nano Letters," Nano Lett. **10**(10), 3816–3822 (2010).
[4] Catchpole, K. R.., Polman, A., "Plasmonic solar cells," Opt. Express **16**(26), 21793 (2008).
[5] Nakayama, K., Tanabe, K.., Atwater, H. A., "Plasmonic nanoparticle enhanced light absorption in GaAs solar cells," Appl. Phys. Lett. **93**(12), 121904 (2008).
[6] Atwater, H. A.., Polman, A., "Plasmonics for improved photovoltaic devices," Nat. Mater. **9**(3), 205–213 (2010).

[7] Ferry, V. E., Verschuuren, M. A., Li, H. B. T., Verhagen, E., Walters, R. J., Schropp, R. E. I., Atwater, H. A.., Polman, A., "Light trapping in ultrathin plasmonic solar cells," Opt. Express **18**(S2), A237–A245 (2010).
[8] Aubry, A., Lei, D. Y., Fernández-Domínguez, A. I., Sonnefraud, Y., Maier, S. A.., Pendry, J. B., "Plasmonic Light-Harvesting Devices over the Whole Visible Spectrum," Nano Lett. **10**(7), 2574–2579 (2010).
[9] Thomann, I., Pinaud, B. A., Chen, Z., Clemens, B. M., Jaramillo, T. F.., Brongersma, M. L., "Plasmon Enhanced Solar-to-Fuel Energy Conversion," Nano Lett. **11**(8), 3440–3446 (2011).
[10] Munday, J. N.., Atwater, H. A., "Large Integrated Absorption Enhancement in Plasmonic Solar Cells by Combining Metallic Gratings and Antireflection Coatings," Nano Lett. **11**(6), 2195–2201 (2011).
[11] Yu, R., Lin, Q., Leung, S.-F.., Fan, Z., "Nanomaterials and nanostructures for efficient light absorption and photovoltaics," Nano Energy **1**(1), 57–72 (2012).
[12] Raschke, G., Kowarik, S., Franzl, T., Sönnichsen, C., Klar, T. A., Feldmann, J., Nichtl, A.., Kürzinger, K., "Biomolecular Recognition Based on Single Gold Nanoparticle Light Scattering," Nano Lett. **3**(7), 935–938 (2003).
[13] Homola, J., "Present and future of surface plasmon resonance biosensors," Anal. Bioanal. Chem. **377**(3), 528–539 (2003).
[14] Jain, P. K., Huang, X., El-Sayed, I. H.., El-Sayed, M. A., "Review of Some Interesting Surface Plasmon Resonance-enhanced Properties of Noble Metal Nanoparticles and Their Applications to Biosystems," Plasmonics **2**(3), 107–118 (2007).
[15] Anker, J. N., Hall, W. P., Lyandres, O., Shah, N. C., Zhao, J.., Van Duyne, R. P., "Biosensing with plasmonic nanosensors," Nat. Mater. **7**(6), 442–453 (2008).
[16] Chung, T., Lee, S.-Y., Song, E. Y., Chun, H.., Lee, B., "Plasmonic Nanostructures for Nano-Scale Bio-Sensing," Sensors **11**(11), 10907–10929 (2011).
[17] Brolo, A. G., "Plasmonics for future biosensors," Nat. Photonics **6**(11), 709–713 (2012).
[18] Sivanesan, A., Izake, E. L., Agoston, R., Ayoko, G. A.., Sillence, M., "Reproducible and label-free biosensor for the selective extraction and rapid detection of proteins in biological fluids," J. Nanobiotechnology **13**(1), 43 (2015).
[19] De Leebeeck, A., Kumar, L. K. S., de Lange, V., Sinton, D., Gordon, R.., Brolo, A. G., "On-Chip Surface-Based Detection with Nanohole Arrays," Anal. Chem. **79**(11), 4094–4100 (2007).
[20] Gordon, R., Sinton, D., Brolo, A. G.., Kavanagh, K. L., "Plasmonic sensors based on nano-holes: technology and integration," 2008, 695913–695913 – 6.
[21] Eftekhari, F., Escobedo, C., Ferreira, J., Duan, X., Girotto, E. M., Brolo, A. G., Gordon, R.., Sinton, D., "Nanoholes As Nanochannels: Flow-through Plasmonic Sensing," Anal. Chem. **81**(11), 4308–4311 (2009).
[22] Sonntag, M. D., Klingsporn, J. M., Zrimsek, A. B., Sharma, B., Ruvuna, L. K.., Van Duyne, R. P., "Molecular plasmonics for nanoscale spectroscopy," Chem Soc Rev **43**(4), 1230–1247 (2014).
[23] Bantz, K. C., Meyer, A. F., Wittenberg, N. J., Im, H., Kurtuluş, Ö., Lee, S. H., Lindquist, N. C., Oh, S.-H.., Haynes, C. L., "Recent progress in SERS biosensing," Phys. Chem. Chem. Phys. **13**(24), 11551–11567 (2011).
[24] Clark, A. W.., Cooper, J. M., "Nanogap Ring Antennae as Plasmonically Coupled SERRS Substrates," Small **7**(1), 119–125 (2011).
[25] Sharma, B., Frontiera, R. R., Henry, A.-I., Ringe, E.., Van Duyne, R. P., "SERS: Materials, applications, and the future," Mater. Today **15**(1–2), 16–25 (2012).
[26] Yue, W., Wang, Z., Yang, Y., Chen, L., Syed, A., Wong, K.., Wang, X., "Electron-beam lithography of gold nanostructures for surface-enhanced Raman scattering," J. Micromechanics Microengineering **22**(12), 125007 (2012).
[27] Dasgupta, A., Singh, D., Tandon, S., Tripathi, R. P. N.., Pavan Kumar, G. V., "Remote-excitation surface-enhanced Raman scattering with counter-propagating plasmons: silver nanowire-nanoparticle system," J. Nanophotonics **8**(1), 083899–083899 (2013).
[28] Im, H., Bantz, K. C., Lee, S. H., Johnson, T. W., Haynes, C. L.., Oh, S.-H., "Self-Assembled Plasmonic Nanoring Cavity Arrays for SERS and LSPR Biosensing," Adv. Mater. **25**(19), 2678–2685 (2013).
[29] Myoung, N., Yoo, H. K.., Hwang, I.-W., "Surface-enhanced Raman scattering detection of toluene and dichlorobenzene vapors using 1-propanethiol-linked Ag nanoparticles," J. Nanophotonics **8**(1), 083083–083083 (2014).
[30] Bauman, S. J., Debu, D. T., Hill, A. M., Novak, E. C., Natelson, D.., Herzog, J. B., "Optical nanogap matrices for plasmonic enhancement applications," SPIE 9163 Plasmon. Met. Nanostructures Their Opt. Prop. XII **9163**, 91631A – 91631A – 6, San Diego, CA (2014).

[31] Ward, D. R., Hüser, F., Pauly, F., Cuevas, J. C.., Natelson, D., "Optical rectification and field enhancement in a plasmonic nanogap," Nat. Nanotechnol. **5**(10), 732–736 (2010).
[32] Krishnan, J. N., Lee, B. C., Shin, H. J.., Kim, S. K. K., "Fabrication and Characterization of Noble Metal Nanowires for Nanogap Devices," ECS Trans. **25**(41), 41–47 (2010).
[33] Chul Kim, H.., Cheng, X., "Gap surface plasmon polaritons enhanced by a plasmonic lens," Opt. Lett. **36**(16), 3082 (2011).
[34] García-Martín, A., Ward, D. R., Natelson, D.., Cuevas, J. C., "Field enhancement in subnanometer metallic gaps," Phys. Rev. B **83**(19), 193404 (2011).
[35] Chen, X., Ciracì, C., Smith, D. R.., Oh, S.-H., "Nanogap-Enhanced Infrared Spectroscopy with Template-Stripped Wafer-Scale Arrays of Buried Plasmonic Cavities," Nano Lett. **15**(1), 107–113 (2015).
[36] Ward, D. R., Grady, N. K., Levin, C. S., Halas, N. J., Wu, Y., Nordlander, P.., Natelson, D., "Electromigrated Nanoscale Gaps for Surface-Enhanced Raman Spectroscopy," Nano Lett. **7**(5), 1396–1400 (2007).
[37] Natelson, D., Li, Y.., Herzog, J. B., "Nanogap structures: combining enhanced Raman spectroscopy and electronic transport," Phys. Chem. Chem. Phys. **15**(15), 5262–5275 (2013).
[38] Herzog, J. B., Knight, M. W., Li, Y., Evans, K. M., Halas, N. J.., Natelson, D., "Dark Plasmons in Hot Spot Generation and Polarization in Interelectrode Nanoscale Junctions," Nano Lett. **13**(3), 1359–1364 (2013).
[39] Bauman, S. J., Novak, E. C., Debu, D. T., Natelson, D.., Herzog, J. B., "Fabrication of Sub-Lithography-Limited Structures via Nanomasking Technique for Plasmonic Enhancement Applications," IEEE Trans. Nanotechnol. **14**(5), 790–793 (2015).
[40] Bauman, S. J., Debu, D. T.., Herzog, J. B., "Plasmonic structures fabricated via nanomasking sub-10 nm lithography technique," Nanoeng. Fabr. Prop. Opt. Devices XII **9556**, 95560M – 95560M – 7, San Diego, CA (2015).
[41] Bauman, S. J., "Fabrication of Sub-10 nm Metallic Structures via Nanomasking Technique for Plasmonic Enhancement Applications," M.S. Thesis, University of Arkansas (2015).
[42] Ward, D. R., Scott, G. D., Keane, Z. K., Halas, N. J.., Natelson, D., "Electronic and optical properties of electromigrated molecular junctions," J. Phys. Condens. Matter **20**(37), 374118 (2008).
[43] Keijsers, R. J. P., Shklyarevskii, O. I., Hermsen, J. G. H.., Kempen, H. van., "Thin film mechanically controllable break junctions," Rev. Sci. Instrum. **67**(8), 2863–2866 (1996).
[44] Ahmad A. Darweesh., Stephen J. Bauman., Joseph B. Herzog., "Optical enhancement in double-width plasmonic gratings with sub-10 nm nanogaps fabricated with blanket nanomasking technique," Manuscr. Prep. (2016).